DOI: 10.5604/01.3001.0013.7914

Volume 95 • Issue 2 • August 2019

Journal of Achievements in Materials and Manufacturing Engineering

International Scientific Journal published monthly by the World Academy of Materials and Manufacturing Engineering

Investigation of structural-geometric parameters and elemental composition of spherical VT20 alloy powders

Z.A. Duriagina [a,b], O.S. Filimonov [a], V.V. Kulyk [a,*], I.A. Lemishka [a], R. Kuziola [b]

[a] Lviv Polytechnic National University, 12 Bandera St., Lviv, 79013, Ukraine

[b] The John Paul II Catholic University of Lublin, Al. Racławickie 14, 20-950 Lublin, Poland

* Corresponding e-mail address: kulykvolodymyrvolodymyrovych@gmail.com

ABSTRACT

Purpose: Identification of structural-geometrical parameters, technological properties and elemental composition of spherical powders in a wide fraction range with respect to the VT20 alloy has been carried out. This is important for evaluating the optimum filling of a given volume by mixture of powders of different fractions during 3D printing.

Design/methodology/approach: During the investigation of spherical Ti-alloy powders, a comprehensive approach was performed using Scanning Electron Microscopy (SEM), Energy-Dispersive X-ray Spectroscopy (EDS), Dynamic Light Scattering (DLS) and Inductively Coupled Plasma Mass Spectrometry (ICP-MS). The surface morphology of the powders was studied on a Tuescan Vega 3 Scanning Electron Microscope. Using the Quantax energy dispersive spectrometer, element distribution maps were obtained and histograms of element distribution in the investigated powders were constructed. ICP-MS analysis was performed to clarify the elemental composition. DLS analysis using Malvern's Zetasizer Nano-ZS equipment allowed us to determine the functional parameters (hydrodynamic radius – R_h, zeta potential – ζ and specific conductivity) of particles of titanium alloy powder that indirectly indicate a tendency to form conglomerates.

Findings: According to the microscopic examinations, the VT20 alloy powder consists of globular-shaped particles with the lamellar traces on their surfaces. The uniformity of the chemical element distribution within each fraction of the investigated powders was confirmed by EDS, and the full conformity of the powder fractions with the elemental composition of the VT20 alloy was confirmed by ICP-MS. The DLS method allowed to establish that the formation of conglomerates would not occur within the studied fractions of the VT20 alloy powder.

Research limitations/implications: The use of high sensitive investigation methods gives understanding of the mechanisms of fine structure formation and possibility to control the processes of powder coagulation in the stage of electrostatic interactions.

Practical implications: The obtained results can be used for the formation of fine spherical particles of the powder, but at the same time, these technologies can be extended for the particles of non-spherical shape.

Originality/value: The DLS method allowed to establish that the formation of conglomerates would not occur within the studied fractions of the VT20 alloy powder. This, in turn, will improve powder melting during 3D printing. The measured zeta potential values allowed us to reveal mechanisms of fine structure formation and to control the processes of powder coagulation in the stage of electrostatic interactions.

Keywords: Spherical VT20 alloy powders, Structural-geometric parameters, Additive technologies, Fluidity, Bulk density, Hydrodynamic radius

Reference to this paper should be given in the following way:

Z.A. Duriagina, O.S. Filimonov, V.V. Kulyk, I.A. Lemishka, R. Kuziola, Investigation of structural-geometric parameters and elemental composition of spherical VT20 alloy powders, Journal of Achievements in Materials and Manufacturing Engineering 95/2 (2019) 49-56.

MATERIALS

1. Introduction

High-tech industries like mechanical engineering, aircraft building and aerospace manufacturing industry require the manufacturing of products with high operational reliability with minimal energy and resource costs to reduce the cost of final products. It is possible to achieve the desired effect by applying additive technologies that allow to form products of complex configuration that do not require finishing machining operation [1].

The principal materials for the manufacturing with applying the additive technologies (3D printing) are metal powders. Among them, titanium alloy powders are considered to be the most promising because they simultaneously have high rates of specific strength, corrosion and heat resistance. Spherical particles are currently used for 3D printing. This is due to the fact that they can more compactly fill a certain volume and provide the necessary fluidity of the powder composition in the material supply systems [2-5].

It is known that the manufacture of such powders is a complex, expensive and environmentally hazardous process. Its particles should be perfectly spherical, homogeneous in elemental composition with a defect-free surface and no tendency to form conglomerates. Therefore, it is important to study the compatibility of structural-geometric parameters of different fractions of the VT20 titanium alloy powder with the specified requirements [6].

2. Experimental procedure

In this work, scanning electron microscopy (SEM), energy-dispersive X-ray spectroscopy (EDS), dynamic light scattering (DLS), and inductively coupled plasma mass spectrometry (ICP-MS) of spherical powders of VT20 titanium alloy were performed using modern research methods and advanced equipment.

SEM analysis of titanium alloys was performed on a TESCAN VEGA 3 scanning electron microscope in high vacuum with the magnification from 3 to 1 million times [7].

The hydrodynamic radius (R_h), zeta potential (ζ), and conductivity of the titanium powder particles were obtained with dynamic light scattering (DLS) technique using Zetasizer Nano-ZS (Malvern). Of these parameters, the most interesting for us is the parameter ζ. It specifies the degree and nature of the interaction between the particles of the system, and the increasing of its absolute value means that the force of repulsion of the particles from each other increases. An investigated system could be considered as unstable if its ζ magnitude lies in a range of +25 to -25 mV. A system is considered as stable for ζ values greater than +25 mV or smaller than -25 mV [8]. The results of the experiment were processed by "Dispersion Technology Software". The autocorrelation functions were registered from the scattered light recorded at 173º. As a dispersant the deionized water was used [9].

The hydrodynamic radius (R_h) was determined from the Stokes-Einstein equation (1) for a known solvent viscosity (η) and temperature (T). The diffusion coefficient (D) was obtained directly from the experiment.

$$R_h = \frac{kT}{6\pi\eta D} \tag{1}$$

where k is the Boltzmann constant, η is the viscosity of the suspension fluid.

It should be noted that the diffusion coefficient D increases with increasing of temperature T according to the

temperature dependence of the dispersant viscosity. Besides, diffusion processes are affected by the change of the particle radius R_h [10,11]. Therefore, the temperature of the sample should be constant (and known) in order to obtain accurate values of D and R_h.

EDS analysis was performed on an energy-dispersive X-ray spectrometer Quantax manufactured by Brucker with a detector which is a silicon crystal that is cooled by a Peltier element. Signal amplification, recording, and spectrum analysis systems are implemented by computer. The elemental composition of the surface was determined on the selected part of the powder by the analytic method of elemental analysis of the solid substance, which is based on the analysis of the energy of emission of its X-ray spectrum [12,13].

To specify the elemental composition, ICP-MS analysis which has a high sensitivity and ability to determine the concentration of elements in the range up to 10^{-10} % has been performed. The method uses inductively coupled plasma as an ion source and mass spectrometer to identify and detect them. ICP-MS also allows the isotope analysis of the selected ion [14].

To specify the structural-geometric parameters of the VT20 alloy powders, their bulk density and fluidity were determined. The essence of the method is to measure the leakage time and, accordingly, the mass of a certain amount of powder, which in a freely filled state completely fills the capacity of the known volume [15,16].

3. Results and discussion

It is important to explore the surface morphology of spherical particles of the VT20 alloy powder of different fractions in order to solve the problems posed. It is necessary to establish the structural-geometric parameters of their surface.

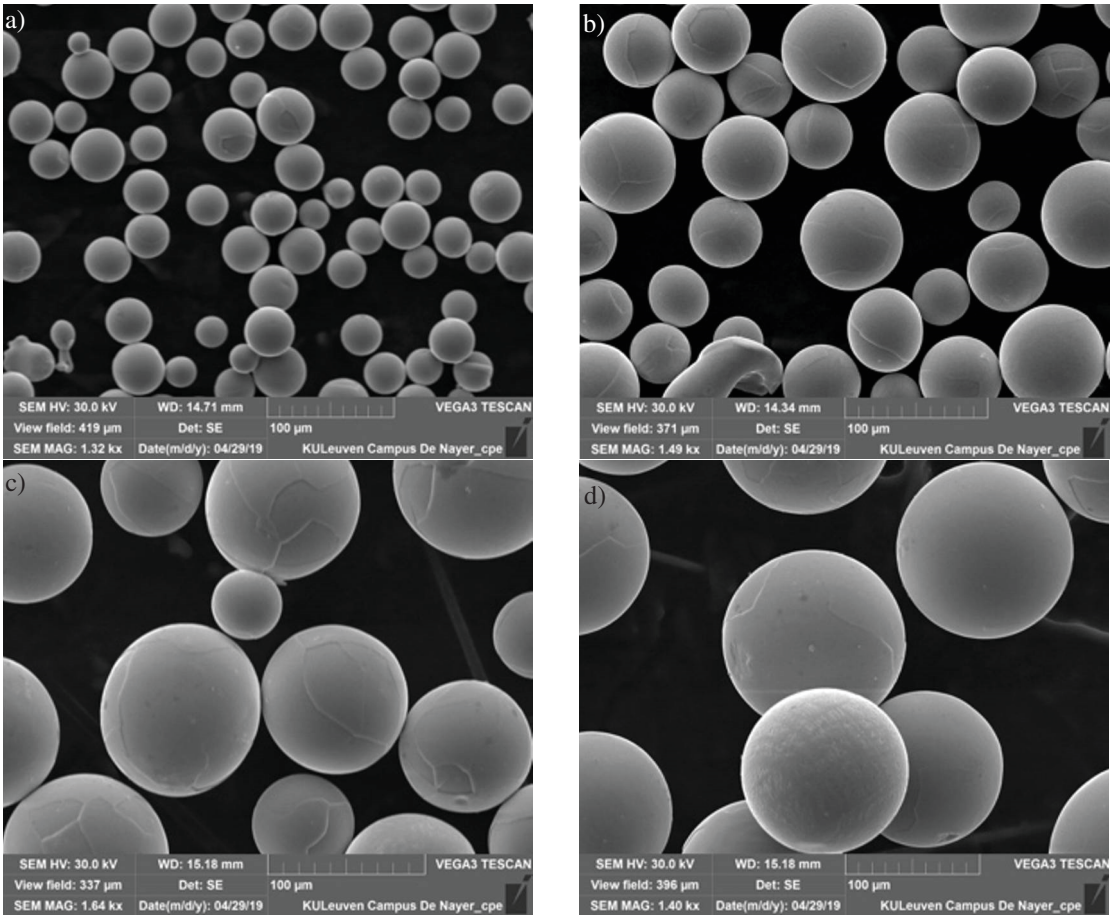

Fig. 1. Surface morphology of spherical particles of the VT20 alloy powder of various fractions: (a) less than 40 µm; (b) 40-80 µm; (c) 80-100 µm; (d) 100-140 µm

According to the results of SEM analysis, the investigated powder consists of globular-shaped particles with the lamellar surface morphology. It is typical of spheroidization technology (Fig. 1).

Figure 2 illustrates the distribution of VT20 alloy powder elements.

The data obtained show that the total distribution of the alloying elements V, Ti, Al (Fig. 2a) on the surface of the powder particles is uniform. Carbon is not detected (Fig. 2b). This indirectly indicates the high quality of the alloy. As expected, the Ti reflex range (Fig. 2c) is the widest. While the nature of the Al distribution is uneven with the areas of liquations (Fig. 2d). Visually, the distribution maps of Zr, V (Fig. 2e, 2f) correspond to their concentrations in the alloy [17].

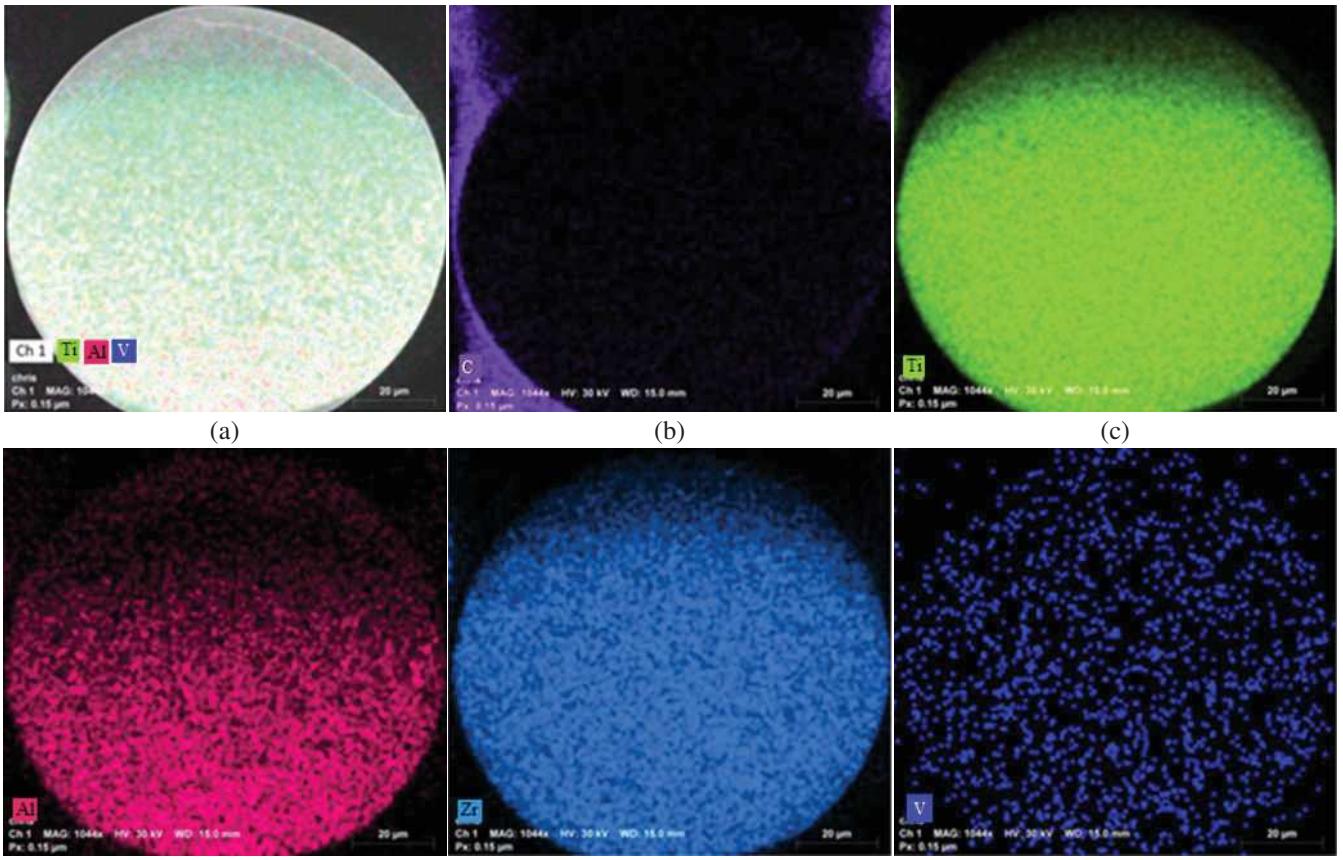

(a) (b) (c)

(d) (e) (f)

Fig. 2. A distribution map of elemental composition of VT20 alloy powder of 80-100 µm fraction: (a) Ti, Al and V; (b) C; (c) Ti; (d) Al; (e) Zr; (f) V

The spectrums of EDS analysis of the fraction 80-100 µm of the VT20 alloy powder are shown in Figure 3.

The percentage range of the elements in the composite mass, visualized in the adequate voltage range, counted in seconds per electron-volt: keV (kilo-electron-volt) is accelerating voltage range used for EDS analysis; cps/eV are counts per second per electron-volt (Fig. 3).

The results of the EDS analysis are shown in Table 1. The received data determines the amount of each element in weight percent on the selected powder area and the relative error of each measurement (σ).

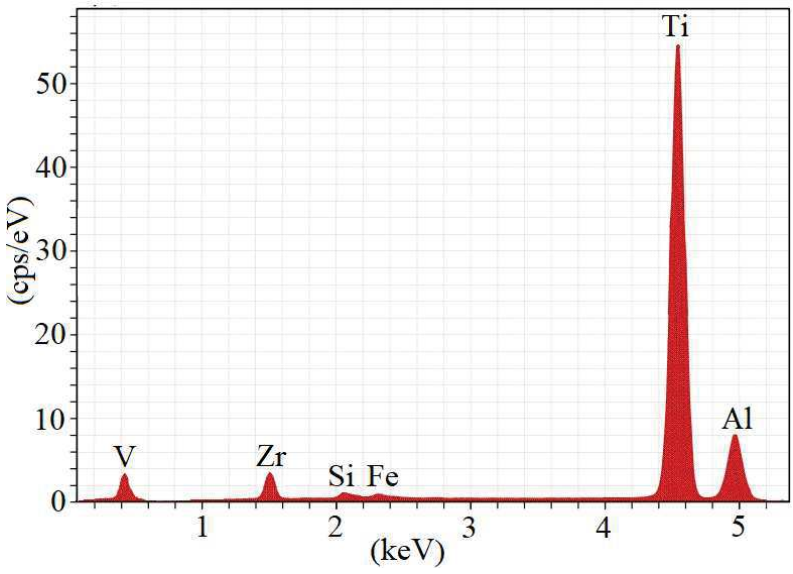

Fig. 3. EDS spectrums of elemental composition of the fraction 80-100 μm of the VT20 alloy powder

Table 1.
Results of EDS analysis

Elements	Wt., %	σ, %
Ti	85.9	1.0
Al	7.7	0.4
Zr	3.2	0.3
V	2.8	0.3
Si	0.4	0.1
Fe	0.3	0.1

ICP-MS analysis was performed to refine the elemental composition up to one hundredth of a percent. Since this mass spectrometer can only process samples in dissolved form, it was necessary to dissolve the test powders in the appropriate reagents. This has been done using CEM Microwave Digestion System MARS 6, and the "Digestion of Titanium Dioxide" program to process the results [18]. The preliminary preparation of the samples for the investigation was in accordance with the procedure specified in the program, namely, 0.5 g of powder with 10 ml of HNO_3 and 2 ml of HF was placed into the digestion vessel for hydrolysis [19]. The test mode is shown in Table 2.

Hydrofluoric acid (HF) was neutralized using the "HF Neutralization" program. The resulting solutions were investigated on a ICP-MS spectrometer. The results of the study are given in Table. 3.

Table 2.
ICP-MS analysis mode

Temp, ºC	Ramp, mm:ss	Hold, mm:ss	Pressure, psi	Power, W	Reagents
210	15:00	15:00	800	900-1050	HNO_3 HF

Table 3.
Results of ICP-MS analysis

Element	Weight, g	mg/100ml	mg/100mg	Wt., %
Al	0.107	5.998	55.935	5.593
Fe	0.107	0.1567	1.465	0.146
Si	0.107	0.2505	2.342	0.234
Ti	0.107	94.925	887.152	88.715
V	0.107	2.708	25.311	2.531
Zr	0.107	2.976	27.815	2.781

It should be noted that, comparing to EDS analysis, ICP-MS analysis allowed to determine the elemental composition of the investigated powders with high

accuracy (error did not exceed 0.01%). In this way, the full conformity of the investigated powder with the elemental composition of the VT20 alloy was confirmed [21].

For DLS research, samples were first prepared 2 mg of prepared powders were suspended in 1ml of deionized water. From the resulting solution 100 µl of the supernatant was taken and again dissolved in 1 ml of deionized water. The final prepared solution was investigated by the DLS installation. The same solution was used to determine the zeta potential and electrophoretic mobility of Ti particles [20]. The values of hydrodynamic radius (R_h), zeta potential (ζ), and specific conductivity are shown in Table 4. The R_h values presented are averages of 10 measurements.

Table 4.
The size of the spherical particles of powders of VT20 titanium alloy, determined by the DLS method

The parameters of the investigated powders	The size of the fraction of spherical powders, µm			
	0-40	40-80	80-100	100-140
R_h, nm	16.5	32.5	46	63
ζ, mV	-29.5	-30.3	-32.9	-26.8
Conductivity, mS/cm	0.0451	0.092	0.0612	0.0504

Since the absolute values of ζ are than 25 mV, this means that the investigated system is stable and the fine powder particles will not form conglomerates [8].

The results of determining the bulk density of powders of VT20 titanium alloy of fractions 0-40, 40-80, 80-100, and 100-140 µm are presented in Table 5. Before the test, we weighed an empty measuring container, and then filled the container with powder. The tests were performed separately for each test sample [15-16].

Table 5.
Results of determination of the fluidity and bulk density of the powders

Powder properties	The fractions of spherical powders, µm			
	0-40	40-80	80-100	100-140
Fluidity (τ), s	47.2	46.5	45.7	45.2
Bulk density (ρ), $\frac{g}{cm^2}$	2.609	2.59	2.57	2.411

Based on the obtained data it was concluded that both the fluidity and bulk density decrease with increasing of the fraction size values.

4. Conclusions

1. The results of microscopic examinations revealed the lamellar traces on surfaces of spherical particles of the VT20 alloy powder. This is typical of a slight temperature difference during the spheroidization process.
2. EDS analysis confirmed the uniformity of the chemical element distribution within each fraction of the investigated powders.
3. ICP-MS confirmed the full conformity of the powder fractions with the elemental composition of the VT20 alloy.
4. The DLS method allowed to establish that the formation of conglomerates would not occur within the studied fractions of the VT20 alloy powder. This, in turn, will improve powder melting during 3D printing. The measured zeta potential values allowed us to reveal mechanisms of fine structure formation and to control the processes of powder coagulation in the stage of electrostatic interactions.

Acknowledgements

The authors would like to show their gratitude to the colleagues from Faculty of Engineering Science, KU Leuven and personally to Prof. Kim Vanmeensel who provided technical support of the research. The authors are also immensely grateful to them for their comments on an earlier version of the manuscript.

References

[1] S. Moylan, E. Whitenton, B. Lane, J. Slotwinski, Infrared thermography for laser-based powder bed fusion additive manufacturing processes, Proceedings of the 40th Annual Review of Progress in Quantitative Nondestructive Evaluation, AIP Conference Proceedings 1581/1 (2015) 1191-1196, DOI: https://doi.org/10.1063/1.4864956.

[2] M. Chen, X. Li, G. Ji, Y. Wu, Z. Chen, W. Baekelant, K. Vanmeensel, H. Wang, J. Kruth, Novel composite powders with uniform TiB_2 nano-particle distribution for 3D printing, Materials for 3D printing 7/3 (2017) 250. DOI: https://doi.org/10.3390/app7030250.

[3] B. Vrancken, S. Dadbakhsh, R. Mertens, K. Vanmeensel, J. Vleugels, S. Yang, J.-P. Kruth, Selective laser melting process optimization of Ti-Mo-TiC metal matrix composites, CIRP Annals 68/1 (2014) 221-224, DOI: https://doi.org/10.1016/j.cirp.2019.04.120.

[4] R. Tkachenko, Z. Duriagina, I. Lemishka, I. Izonin, A. Trostianchyn, Development of machine learning method of titanium alloy properties identification in additive technologies, Eastern-European Journal of Enterprise Technologies 3/12 (2018) 23-31, DOI: https://doi.org/10.15587/1729-4061.2018.134319.

[5] T.L. Tepla, I.V. Izonin, Z.A. Duriagina, R.O. Tkachenko, A.M. Trostianchyn, I.A. Lemishka, V.V. Kulyk, T.M. Kovbasyuk, Alloys selection based on the supervised learning technique for design of biocompatible medical materials, Archives of Materials Science and Engineering 93/1 (2018) 32-40, DOI: https://doi.org/10.5604/01.3001.0012.6944.

[6] Z.A. Duriagina, R.O. Tkachenko, A.M. Trostianchyn, I.A. Lemishka, A.M. Kovalchuk, V.V. Kulyk, T.M. Kovbasyuk, Determination of the best microstructure and titanium alloy powders properties using neural network, Journal of Achievements of Materials and Manufacturing Engineering 87/1 (2018) 25-31, DOI: https://doi.org/10.5604/01.3001.0012.0736.

[7] N.A. Pohlman, J.A. Roberts, M.J. Gonser, Characterization of titanium powder: microscopic views and macroscopic flow, Powder Technology 228 (2012) 141-148, DOI: https://doi.org/10.1016/j.powtec.2012.05.009.

[8] A. Azouri, K. Xun, K. D. Sattler, Zeta potential studies of titanium dioxide and silver nanoparticle composites in water-based colloidal suspension, Characterization of Nanoparticles 2008 (2008) 221-223, DOI: https://doi.org/10.1115/MN2006-17072.

[9] V. Ruseva, H. Jankev, J. Corbett, An optimized filling method for capillary DLS, MethodsX 6 (2019) 606-614, DOI: https://doi.org/10.1016/j.mex.2019.03.006.

[10] V.G. Navas, A. Sanda, C. Sanz, D. Fernandez, K. Vanmeensel, Surface integrity of rotary ultrasonic machined ZrO_2-TiN and Al_2O_3-TiC-SiC ceramics, Journal of the European Ceramic Society 35/14 (2015) 3927-3941, DOI: https://doi.org/10.1016/j.jeurceramsoc.2015.06.018.

[11] A.V. Minitsky, M.A. Sisoev, N.V. Minitsky, The duration of surface thermal processing and the structure of powdered iron-carbon alloys, Metal Science and Metal Processing 2016 (2016) 3-6 (in Ukrainian).

[12] A.M. Tonejc, I. Djerdj, A. Tonejc, Evidence from HRTEM image processing, XRD and EDS on nanocrystalline iron-doped titanium oxide powders, Materials Science and Engineering: B 85/1 (2019) 397-417, DOI: https://doi.org/10.1016/S0921-5107(01)00641-9.

[13] V.-D. Hodoroaba, Chapter 4.4 – Energy-dispersive X-ray spectroscopy (EDS), in: V.-D. Hodoroaba, W.E.S. Unger, A.G. Shard (Eds.), Characterization of Nanoparticles. Measurement Processes for Nanoparticles. Micro and Nano Technologies, Elsevier, 2016, 186-273, DOI: https://doi.org/10.1016/B978-0-12-814182-3.00021-3.

[14] B. Bocca, S. Caimi, Oreste Senofonte, A. Alimonti, F. Petrucci, ICP-MS based methods to characterize nanoparticles of TiO_2 and ZnO in sunscreens with focus on regulatory and safety issues, Science of The Total Environment 630 (2018) 922-930, DOI: https://doi.org/10.1016/j.scitotenv.2018.02.166.

[15] ISO ISO 3923-1:2018, Metallic powders. Determination of apparent density. Part 2: Scott volumeter method, 2018, 2-4.

[16] ISO 4490:2018, Metallic powders. Determination of flowability by means of a calibrated funnel (Hall flowmeter), 2018, 5-6.

[17] Z.A. Duriagina, I.A. Lemishka, A.M. Trostianchyn, V.V. Kulyk, S.G. Shvachko, T.L. Tepla, E.I. Pleshakov, T.M. Kovbasyuk, The effect of morphology and particle-size distribution of VT20 titanium alloy powders on the mechanical properties of deposited coatings, Powder Metallurgy and Metal Ceramics 57 (2019) 697-702, DOI: https://doi.org/10.1007/s11106-019-00033-8.

[18] C. Huang, Z. Jiang, B. Hu, Mesoporous titanium dioxide as a novel solid-phase extraction material for flow injection micro-column preconcentration on-line coupled with ICP-OES determination of trace metals in environmental samples, Talanta 73/2 (2007) 274-281, DOI: https://doi.org/10.1016/j.talanta.2007.03. 046.

[19] L. Bolzoni, E.M. Ruiz-Navas, E. Neubauer, E. Gordo, Inductive hotpressing of titanium and titanium alloy powders, Materials Chemistry and Physics 131 (2012)

672-679, DOI: https://doi.org/10.1016/j.matchemphys.2011.10.034.

[20] C.R.F. Azevedo, D. Rodrigues, F.B. Neto, Ti-Al-V powder metallurgy (PM) via the hydrogenation–dehydrogenation (HDH) process, Journal of Alloys and Compounds 353 (2003) 217-227, DOI: https://doi.org/10.1016/S0925-8388(02)01297-5.

[21] H.M. Sakho, E. Allahyari, O.S. Oluwafemi, S. Thomas, Chapter 2 – Dynamic Light Scattering (DLS), in: S. Thomas, R. Thomas, A.K. Zachariah, R.K. Mishra (Eds.), Thermal and Rheological Measurement Techniques for Nanomaterials Characterization. Micro and Nano Technologies, Elsevier, 2017, 37-49. DOI: https://doi.org/10.1016/ B978-0-323-46139-9.00002-5.